

Topochemical and morphological characterization of wood cell wall treated with the ionic liquid, 1-ethylpyridinium bromide

Toru Kanbayashi · Hisashi Miyafuji

Received: 15 October 2014 / Accepted: 18 December 2014 / Published online: 3 January 2015
© Springer-Verlag Berlin Heidelberg 2014

Abstract

Main conclusion [EtPy][Br] is more reactive toward lignin than toward the PSs in wood cell walls, and [EtPy][Br] treatment results in inhomogenous changes to the cell wall's ultrastructural and chemical components.

The effects of the ionic liquid 1-ethylpyridinium bromide ([EtPy][Br]), which prefers to react with lignin rather than cellulose on the wood cell walls of Japanese cedar (*Cryptomeria japonica*), were investigated from a morphology and topochemistry point of view. The [EtPy][Br] treatment induced cell wall swelling, the elimination of warts, and the formation of countless pores in the tracheids. However, many of the pit membranes and the cellulose crystalline structure remained unchanged. Raman microscopic analyses revealed that chemical changes in the cell walls were different for different layers and that the lignin in the compound middle lamella and the cell corner resists interaction with [EtPy][Br]. Additionally, the interaction of [EtPy][Br] with the wood cell wall is different to that of other types of ionic liquid.

Keywords 1-Ethylpyridinium bromide · Cell wall · Ionic liquid · Microscopy · Raman microscopy · Wood

Abbreviations

CC	Cell corner
CML	Compound middle lamella
[C2mim][Cl]	1-Ethyl-3-methylimidazolium chloride
[EtPy][Br]	1-Ethylpyridinium bromide
PSs	Polysaccharides
S ₂	Middle layer of secondary wall
S ₃	Inner layer of secondary wall
SEM	Scanning electron microscopy

Introduction

With increased concern about global warming and fossil resource exhaustion, lignocellulosics have attracted much attention as an alternative to fossil resources. Woody biomass is regarded as a promising resource because it is carbon neutral, widely available and does not compete with food supply. Much research has been conducted on converting woody biomass into fossil resource alternatives (Piskorz et al. 1988; Mok and Antal 1992; Taherzadeh et al. 1997; Yamazaki et al. 2006; Zhao et al. 2008), and ionic liquids have been vigorously studied as a pretreatment for the chemical conversion of woody biomass (Lee et al. 2009).

Ionic liquids have been the subject of intense study in many fields since the discovery of air and water-stable ionic liquids (Wilkes and Zaworotko 1992). Ionic liquids are defined as organic salts with a low melting point (around or below 100 °C). They have many remarkable properties such as no detectable vapor pressure, low viscosity and high thermal stability. They can dissolve a wide range of organic and inorganic compounds (Seddon 1997; Sheldon 2001; Rogers and Seddon 2003). Additionally, ionic liquids can be designed as solvents for certain

Special topic: Polyphenols: biosynthesis and function in plants and ecosystems. Guest editor: Stefan Martens.

T. Kanbayashi · H. Miyafuji (✉)
Division of Environmental Sciences, Graduate School of Life and Environmental Sciences, Kyoto Prefectural University, Hangi-cho, Shimogamo, Sakyo-ku, Kyoto 606-8522, Japan
e-mail: miyafuji@kpu.ac.jp

reactions by the selection of suitable cations and anions. Therefore, they can be thought of as “designer solvents” (Freemantle 1998). The high solubility and reusability of ionic liquids are very attractive properties and, therefore, ionic liquids show great promise as new reaction solvents (Earle and Seddon 2000).

Recently, it has been found that certain ionic liquids have the ability to dissolve cellulose (Swatloski et al. 2002; Zhang et al. 2005; Kosan et al. 2008) and even wood (Honglu and Tiejun 2006; Fort et al. 2007; Kilpeläinen et al. 2007). Ionic liquid technology has subsequently been developed for the efficient use of woody biomass. The interaction of wood with ionic liquids has gradually been clarified from chemical (Miyafuji et al. 2009; Nakamura et al. 2010a, b), topochemical (Kanbayashi and Miyafuji 2014b; Zhang et al. 2014), and morphological (Lucas et al. 2011; Viell and Marquardt 2011; Miyafuji and Suzuki 2012; Kanbayashi and Miyafuji 2013, 2014a) points of view. As in the references given above, imidazolium-based ionic liquids are mainly used in this research field and few studies exist on the use of other types of ionic liquids. Our earlier research on liquefaction of wood by ionic liquids revealed that both 1-ethyl-3-methylimidazolium chloride ([C2mim][Cl]) and 1-ethylpyridinium bromide ([EtPy][Br]) can liquefy all components of wood although the reaction rate of the wood components with these ionic liquids is different for the types of ionic liquids. The yield of residue of western red cedar after treatment with [C2mim][Cl] at 120 °C for 8 h can be reduced to 30 %, and the decrease in yield of residue was caused mainly by decrease in the amount of cellulose (Nakamura et al. 2010a). On the other hand, the yield of residue of Japanese cedar after treatment with [EtPy][Br] at 120 °C for 24 h can be reduced to 43 %, and the decrease in yield of residue was caused mainly by decrease in the amount of lignin (Yokoo and Miyafuji 2014). However, little is known about the interaction of wood with ionic liquids with respect to the pyridinium-based ionic liquids. For a better understanding of the effects of the pyridinium-based ionic liquid [EtPy][Br], we investigated the morphological and chemical changes in wood cell walls after treatment with [EtPy][Br]. Light microscopy and scanning electron microscopy (SEM) were used to observe morphological changes. Raman microscopy was employed to investigate spectral changes in the different types of layers and to visualize chemical changes in the cell wall during [EtPy][Br] treatment.

Materials and methods

Samples and chemicals

Japanese cedar (*Cryptomeria japonica*) samples were cut to make blocks (approx. 5(R) × 5(T) × 5(L) mm) that were

then extracted with ethanol/benzene (1:2, v/v) for 8 h in a Soxhlet apparatus. The extracted wood was oven dried at 105 °C for 24 h before use. 1-Ethylpyridinium bromide ([EtPy][Br]) was purchased from Tokyo Chemical Industry Co., Ltd., Japan.

Light microscopy analysis

The extracted wood samples were cut with a sliding microtome into 15- μ m-thick sections and mounted in a 20- μ m-deep hemocytometer (Sunlead Glass Corp., Saitama, Japan). All mounted sections were dried for 2 h at 105 °C before adding 100 μ L of [EtPy][Br] that was heated to 120 °C by dropping the ionic liquid onto the mounted section. The hemocytometer was closed with a cover glass immediately after adding the ionic liquid. This was designated as the beginning of the treatment. The hemocytometer was placed in an oven at 120 °C for various time periods and then removed from the oven to examine anatomical changes in the wood section using light microscopy (BH-2, Olympus). Three areas (cell lumen area, cell wall area, and total of cell lumen area + cell wall area; defined as shown in Fig. 1) were measured for five neighboring cells in the late- and earlywood, using image analysis software (Motic Image Plus 2.2S, Shimadzu Rika Corporation, Tokyo, Japan) and the average was calculated for each area.

Scanning electron microscopy (SEM) observations

Extracted wood samples were surfaced with a sliding microtome. The surfaced samples were dried for 24 h at 105 °C and the surfaced area was treated by dipping into [EtPy][Br] and heating to 120 °C for various periods of time. During dipping treatment the [EtPy][Br] was stirred gently with a magnetic stirrer. The treated specimens were dipped in dimethylsulfoxide (DMSO) to remove [EtPy][Br] and then washed with distilled water to remove DMSO. After drying for 24 h at 105 °C, each specimen was

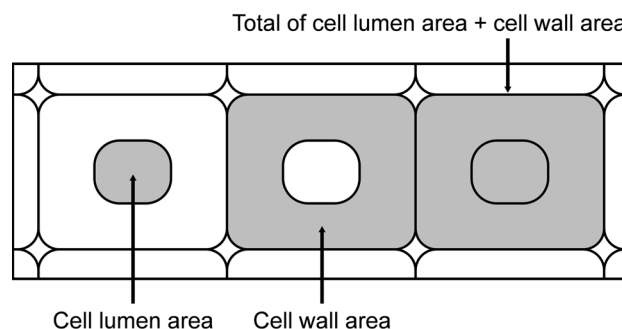


Fig. 1 Definition of the cell lumen area, the cell wall area, and the total of the cell lumen area + the cell wall area

mounted on a specimen holder and then Au coated. The exposed surface was examined by SEM (JSM-5510LV, JEOL, Tokyo, Japan) at an accelerating voltage of 10 kV. No morphological changes in the wood cells because of this accelerating voltage were observed.

Raman microscopy analysis

For Raman microscopy the [EtPy][Br] treatment was the same as that for light microscopy. To perform analysis on the same cell wall area with respect to Raman mapping, 15- μm -thick serial sections were prepared. After a specific treatment time, a large amount of distilled water was poured into the hemocytometer from its lateral direction, and then the hemocytometer was placed in a Petri dish filled with distilled water for 24 h at room temperature to completely remove [EtPy][Py].

Raman analyses were performed with a confocal microRaman system (LabRAM ARAMIS, Horiba Jobin Yvon, Longjumeau, France) equipped with a confocal microscope (BX41, Olympus) and a motorized x, y stage. For high spatial resolution, the measurements were conducted with a high numerical aperture ($\text{NA} = 1.40$) oil immersion microscope objective (UPLSAPO 100XO, Olympus) and a 532 nm diode-pumped solid state laser (Ventus VIS 532, Laser Quantum, Cheshire, UK). The theoretical lateral resolution on the sample was about 0.23 μm ($0.61\lambda/\text{NA}$) where λ is the wavelength of the laser and NA is the numerical aperture of the microscope objective. The incident laser power on the sample was approximately 10 mW. Scattered Raman light was detected by a charge-coupled device (CCD) detector behind either a 300 or 1,800 lines/mm grating. A confocal pinhole diameter of 300 μm was used for all experiments.

To obtain high-quality spectra and avoid damaging the wood samples by the heat of the laser during the point analysis, the Raman spectra were measured in ten cycles with each cycle consisting of a 1 s integration time for one

spot. Ten spectra were obtained and averaged and these averaged spectra from ten different locations were again averaged. The grating used in the point analysis was 1,800 lines/mm. For mapping analysis, measurements were conducted every 0.4 μm and the spectra were obtained by averaging four cycles, each with a 0.2 s integration time. The grating used for mapping was 300 lines/mm.

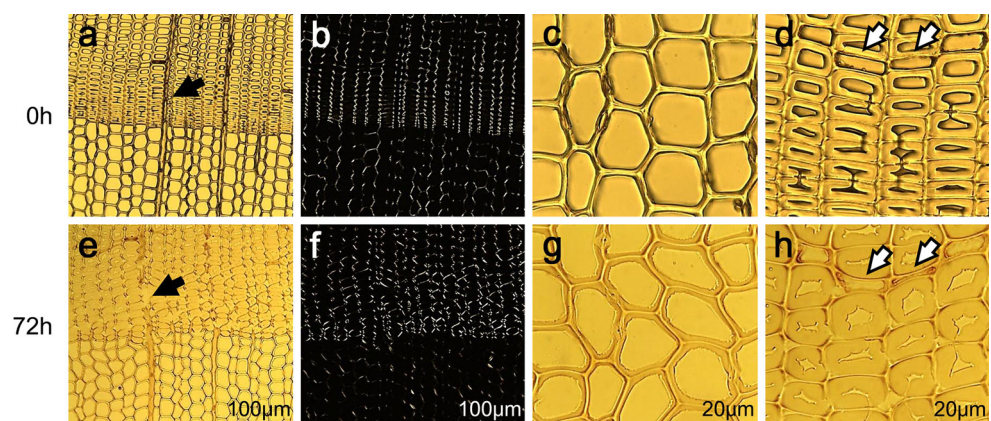
LabSpec5 software (Horiba Jobin Yvon) was used for data acquisition and analysis. To remove the fluorescence background, the raw spectral data were baseline corrected. Smoothing to reduce spectral noise was done using the Savitsky–Golay algorithm.

Results and discussion

Morphological characterization using light microscopy and SEM

The light micrographs revealed the morphology of the cell walls in [EtPy][Br]. Figure 2 shows light microscopy and polarized light microscopy images of a transverse section before and after treatment for 72 h with [EtPy][Br] at 120 °C. The cell walls of the tracheids were swollen and the structure was slightly disordered. However, they were hardly dissociated in both the late- and earlywood after [EtPy][Br] treatment (Fig. 2e, g, h). In our earlier research into morphological changes during 1-ethyl-3-methylimidazolium chloride ([C2mim][Cl]) treatment, the cell walls of Japanese cedar tracheids were found to be dissociated in the latewood, but not in the earlywood (Miyafuji and Suzuki 2012). For the other tissues the ray parenchyma cells were partly destroyed in the latewood, but not in the earlywood (indicated by filled arrows), and the axial parenchyma cells collapsed on the cell lumen side (indicated by open arrows). These morphological changes in the parenchyma cells were triggered by pressure from neighboring swollen tracheids. From polarized light microscopy

Fig. 2 Light microscopy and polarized light microscopy images of a transverse section before and after treatment for 72 h with [EtPy][Br] at 120 °C. **a, e** Around the annual ring boundary. **b, f** Polarized light microscopy images of **a** and **e**. **c, g** Magnified view of the earlywood. **d, h** Magnified view of the latewood. *Filled arrow* ray parenchyma cell, *open arrow* axial parenchyma cell



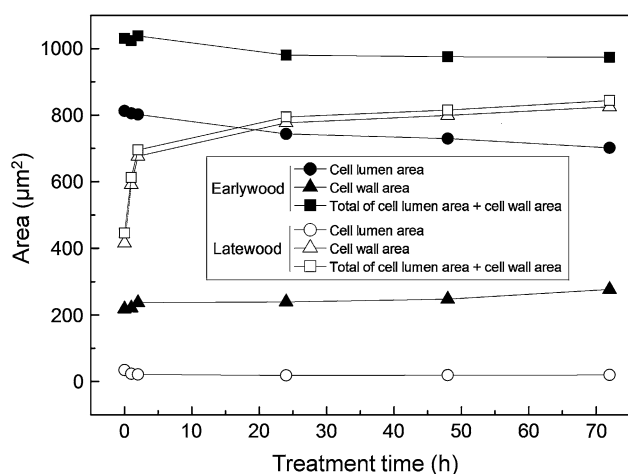


Fig. 3 Changes in the cell wall area, the cell lumen area, and the total of the cell lumen area + the cell wall area during [EtPy][Br] treatment

observations, the brightness from the birefringence of cellulose did not change after [EtPy][Br] treatment (Fig. 2f). This result indicates that the crystalline structure of cellulose in the wood cell walls was preserved after treatment for 72 h with [EtPy][Br] at 120 °C.

To analyze the swelling behavior of the tracheids during [EtPy][Br] treatment in detail, time sequential measurements of the cell wall area, the cell lumen area, and the total cell lumen area + cell wall area (defined in Fig. 1) were obtained using image analysis software. The results are shown in Fig. 3. During the initial stages of [EtPy][Br] treatment, all the measured areas in the earlywood only changed slightly. The cell wall area and the total of the cell lumen area + the cell wall area in the latewood increased significantly. Thereafter, the changes varied. In the latewood, although the cell wall area and the total of the cell lumen area + the cell wall area increased gradually with an increase in treatment time, the cell lumen area hardly changed. In the earlywood the cell wall area increased slightly, but the total cell lumen area + the cell wall area and the cell lumen area decreased. This decrease is caused by the deformation of the cell walls because of pressure from the swelling of the cell walls in the latewood. After 72 h of treatment, the cell wall areas in the earlywood and the latewood increased 1.3 and 2 times, respectively. In our previous study, we reported that the cell wall areas in the latewood of the tracheids of Japanese cedar increased five times after treatment for 48 h with [C2mim][Cl] (Miyafuji and Suzuki 2012). These results indicate that the swelling efficiency of [EtPy][Br] in the cell walls is lower than that of [C2mim][Cl], and morphological changes in the cell walls are different for each type of ionic liquid.

The SEM images in Fig. 4 show ultrastructural changes in the various cell wall structures before and after treatment

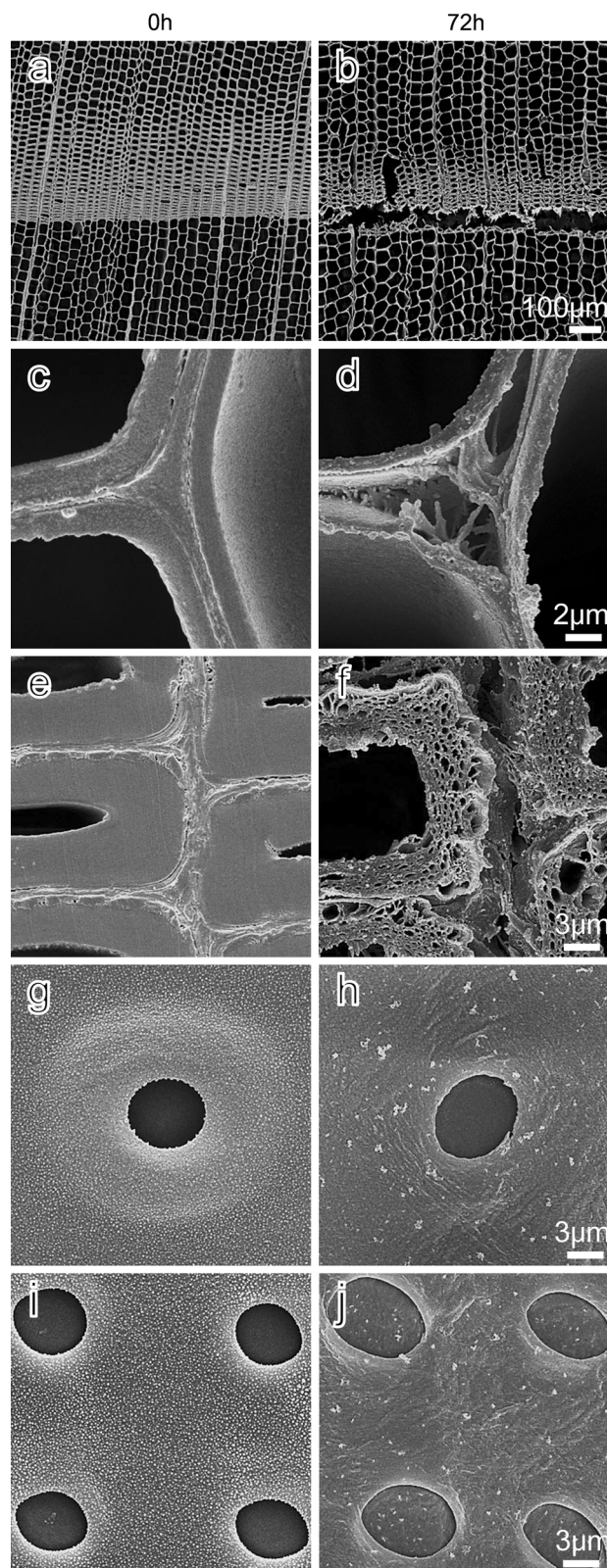


Fig. 4 SEM images of various tissues before and after treatment for 72 h with [EtPy][Br] at 120 °C. **a, b** Around the annual ring boundary. **c, d** Magnified view of the earlywood. **e, f** Magnified view of the latewood. **g, h** Bordered pits. **i, j** Taxodioid pits

Table 1 Raman bands used for the analysis and their PSs assignment (PS; cellulose and/or hemicellulose) and lignin (L)

Raman band (cm ⁻¹)	Component	Band assignment ^a
3,074	L	Aromatic C–H stretch
2,941	L	C–H stretch in OCH ₃ (asymmetric)
2,894	PS	C–H and C–H ₂ stretching
2,850	L	C–H stretch in OCH ₃ (symmetric)
1,656	L	C=C coniferyl alcohol + C=O coniferyl aldehyde
1,620	L	C=C stretch of coniferyl aldehyde
1,596	L	Aromatic ring stretch (symmetric)
1,453	PS, L	HCH and HOC bending, CH ₃ bending in OCH ₃
1,377	PS	HCC, HCO, and HOC bending
1,336	L	Aliphatic O–H bend
1,272	L	Aryl–O of aryl–OH and aryl–O–CH ₃ ; guaiacyl ring (with C=O group) mode
1,193	L	A phenol mode
1,151	PS	Heavy atom (CC and CO) stretching, HCC and HCO bending
1,138	L	A mode of coniferyl aldehyde
1,122	PS	C–O–C stretch (symmetric)
1,096	PS	C–O–C stretch (asymmetric)
920	L	CCH wag
899	PS, L	HCC and HCO bending at C6, skeletal deformation
785	L	Skeletal deformation
731	L	Skeletal deformation
591	L	Skeletal deformation
457	PS, L	Some heavy atom stretching, skeletal deformation
381	PS	Some heavy atom stretching

^a Assignments based on literature (Wiley and Atalla 1987; Agarwal and Ralph 1997, 2008; Edwards et al. 1997; Agarwal 1999; Schenzel and Fischer 2001; Agarwal et al. 2011)

for 72 h with [EtPy][Br] at 120 °C. After the 72 h treatment, cracks were observed around the annual ring boundary (Fig. 4b). Additionally, large parts of the compound middle lamella (CML) and the cell corner (CC) disappeared in both the earlywood and the latewood (Fig. 4d, f). The surface of the middle layer of the secondary wall (S₂) was full of large pores in the latewood (Fig. 4f). The observed cracks and the disappearance of the CML and the CC were not evident by light microscopy and these changes may thus be attributed to a shrinkage of the cell wall structure during SEM pretreatment, likely in the drying process. The disappearance of the CML and the CC may also be related to lignin distribution in the wood cells. The CML and the CC regions contain more than 50 and 70 % lignin, respectively, whereas the S₂ region contains about 20 % lignin (Donaldson 2001). Our recent study revealed that lignin can be liquefied more rapidly than cellulose by [EtPy][Br] (Yokoo and Miyafuji 2014). Therefore, a significant liquefaction and elution of chemical components occurred in the CML and the CC regions, and these regions, in which the volume decreased, shrunk significantly upon subsequent drying. The formation of pores in the transverse section's surface of the secondary

wall has also been observed during chemical and physicochemical treatments such as an alkaline treatment (Ji et al. 2014), steam explosion (Corrales et al. 2012), and ammonia fiber expansion (AFEX) (Chundawat et al. 2011). The formation of large pores may be associated with the partial liquefaction and elution of chemical components, particularly lignin; however, the details still require further investigation.

As shown in Fig. 4h, j, the pit membranes in the bordered pits and in the taxodioid pits hardly changed. Most of the warts on the surface of the tracheids (Fig. 4g, i) disappeared after [EtPy][Br] treatment. The pit membranes are mainly composed of cellulose microfibrils (Harada and Côté 1985), whereas the warts are chemically composed of lignin and hemicellulose (Jansen et al. 1998). The difference in the reactivity of [EtPy][Br] with these tissues comes from their different chemical components.

Topochemical characterization using Raman microscopy

Raman spectra of the tracheids treated with [EtPy][Br] at 120 °C for 0, 24, and 72 h were obtained for the S₂, the

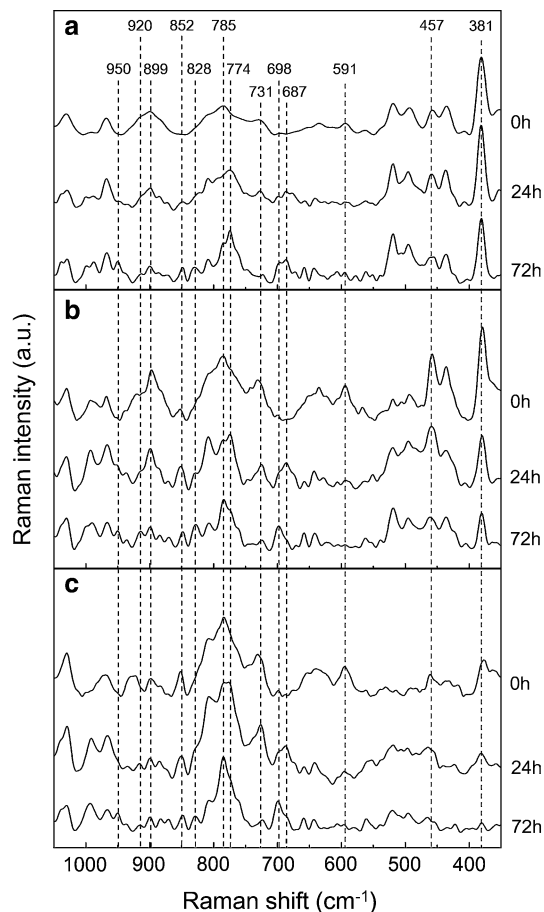


Fig. 5 Raman spectra for S_2 (a), CML (b) and CC (c) of the tracheids before and after treatment with [EtPy][Br] at 120 °C for 0, 24, and 72 h; enlargement of the spectral region from 350 to 1,050 cm^{-1}

CML, and the CC regions. Spectra from 350 to 3,150 cm^{-1} were studied because this spectral range includes bands from the components of wood including cellulose, hemicellulose, and lignin. However, no spectral features were found between 1,710 and 2,750 cm^{-1} before or after treatment with [EtPy][Br]. Therefore, this region is not shown here. The Raman spectral features of cellulose are very similar to those of hemicellulose. The hemicellulose band is broader and can reside beneath the cellulose band, because less hemicellulose is present and it is less crystalline (Agarwal and Ralph 1997). Therefore, bands from cellulose and hemicellulose cannot be distinguished and they are referred to as polysaccharides (PSs) in this study. The peak assignments discussed in this paper are summarized from previous reports and shown in Table 1.

Point analysis

The Raman spectra were divided into four regions: from 350 to 1,050 cm^{-1} (Fig. 5), from 1,050 to 1,540 cm^{-1} (Fig. 6), from 1,540 to 1,710 cm^{-1} (Fig. 7) and from 2,750

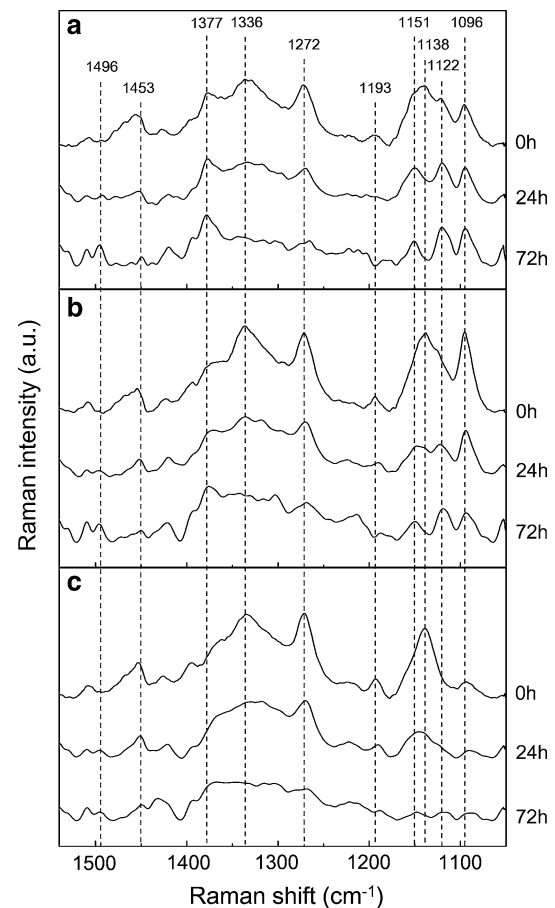


Fig. 6 Raman spectra for S_2 (a), CML (b), and CC (c) of the tracheids before and after treatment with [EtPy][Br] at 120 °C for 0, 24, and 72 h; enlargement of the spectral region from 1,050 to 1,540 cm^{-1}

to 3,150 cm^{-1} (Fig. 8). Each region is discussed in detail below.

Region from 350 to 1,050 cm^{-1}

The bands in this spectral region have not all been assigned but the bands of components such as the PSs and lignin are known. A decrease in band intensity was observed at 591, 731, and 920 cm^{-1} for the whole cell wall area. All these peaks, with decreased intensity, are assigned to lignin. Other lignin bands were observed at 457, 785, and 899 cm^{-1} . However, these bands partially overlap with the PSs bands. Changes in the intensity of these bands differed among the respective cell wall areas. For example, the band intensity at 457 cm^{-1} only changed slightly for the S_2 during the treatment, whereas it decreased for the CML and the CC with an increase in the treatment time. Additionally, the band at 381 cm^{-1} , which is only assigned to cellulose, decreased significantly for the CML and the CC after the 72 h treatment. These differences in spectral

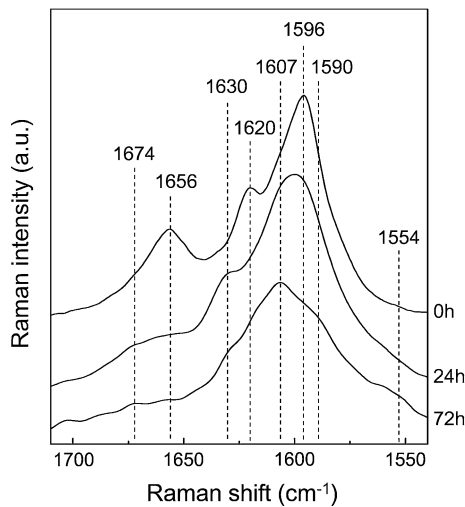


Fig. 7 Raman spectra for CML of the tracheids before and after treatment with [EtPy][Br] at 120 °C for 0, 24, and 72 h; enlargement of the spectral region from 1,540 to 1,710 cm^{-1}

changes among the S_2 , the CML, and the CC indicate that the reactivity of [EtPy][Br] in wood cell walls is inhomogeneous.

Several new peaks were observed at 687, 774, 828, and 950 cm^{-1} . The band intensity at 687 and 774 cm^{-1} increased for the CML and the CC after the 24 h treatment and decreased after the 72 h treatment, whereas the intensity of these bands continued to increase after 72 h for the S_2 . The band intensity at 698 cm^{-1} , which has not been assigned, increased significantly for all the cell wall areas. A peak at 852 cm^{-1} was observed in both before and after treatment with [EtPy][Br]. This band has not been detected in other wood species (Agarwal and Ralph 1997) and, therefore, this band may be characteristic of Japanese cedar.

Region from 1,050 to 1,540 cm^{-1}

In all the cell wall areas, the band intensities at 1,138, 1,193, 1,272, 1,336, and 1,453 cm^{-1} decreased with an increase in treatment time. Most of these bands can be assigned to lignin. The most significant decrease was at the positions where coniferyl aldehyde (1,138 cm^{-1}) was present. On the other hand, the peaks at 1,122, 1,151, and 1,377 cm^{-1} became sharper after the treatment. All these bands come from the PSs. However, the band intensity at 1,096 cm^{-1} in the CML and the CC decreased gradually with an increase in the treatment time, and this band can be assigned to the PSs. These changes come from a decrease in the peripheral lignin bands. From these results, lignin preferentially reacts with [EtPy][Br] compared with the PSs in wood cell walls. This result is similar to our pre-

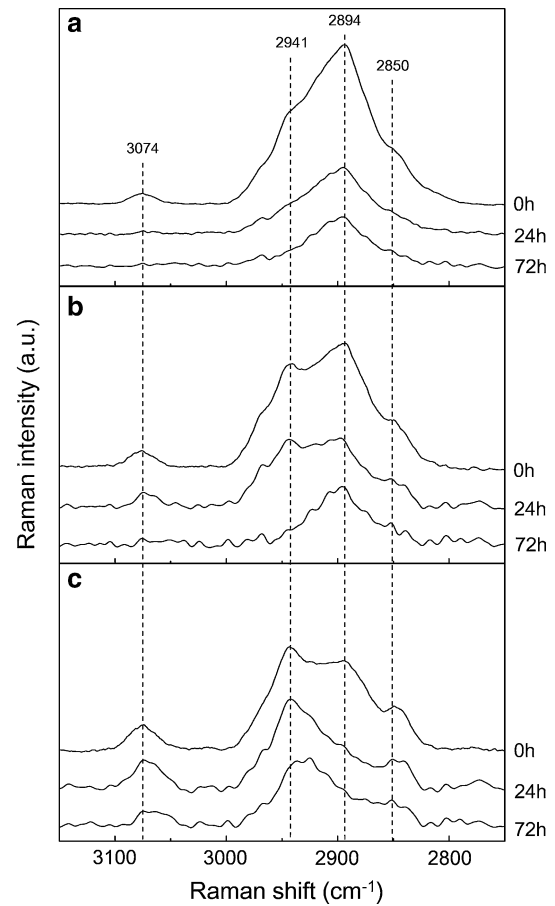


Fig. 8 Raman spectra for S_2 (a), CML (b), and CC (c) of the tracheids before and after treatment with [EtPy][Br] at 120 °C for 0, 24, and 72 h; enlargement of the spectral region from 2,750 to 3,150 cm^{-1}

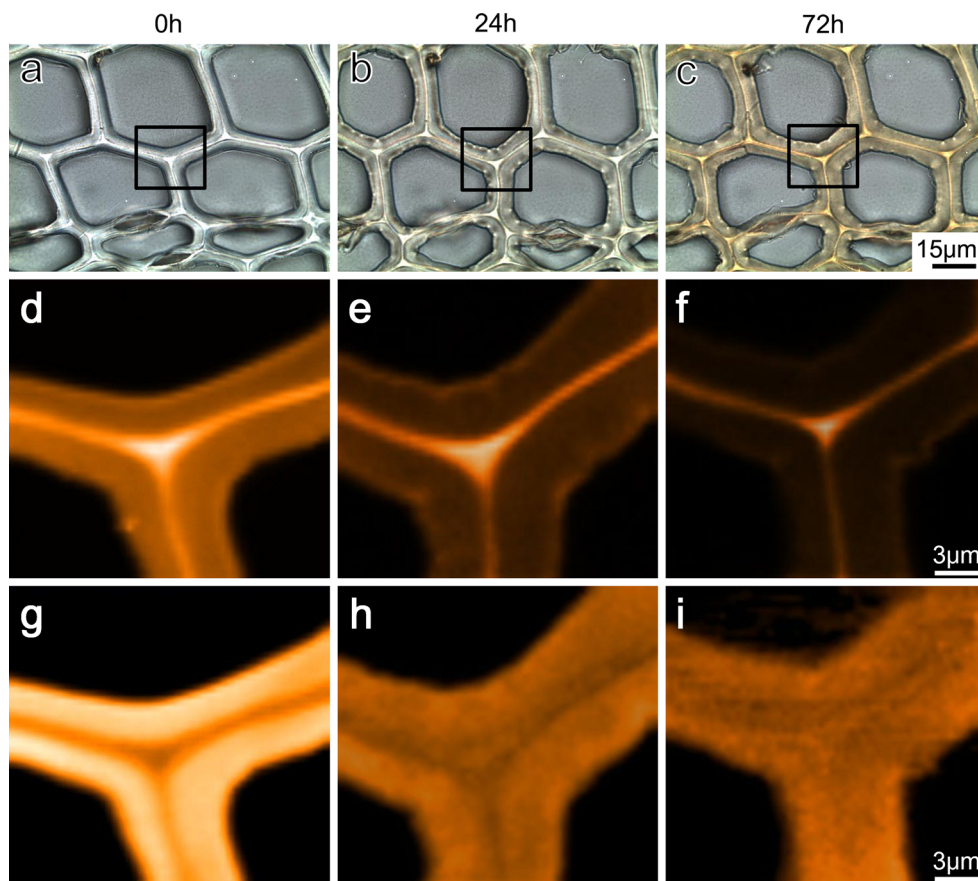
vious paper on liquefaction of the wood flour of Japanese cedar by [EtPy][Br] which reported that lignin can be easily liquefied in [EtPy][Br] than cellulose (Yokoo and Miyafuji 2014).

A new band appeared at 1,496 cm^{-1} , and this band's intensity increased as the treatment time increased. This change is similar to our previous report on the treatment of wood with the ionic liquid, 1-ethyl-3-methylimidazolium chloride ([C2mim][Cl]) (Kanbayashi and Miyafuji 2014b).

Region from 1,540 to 1,710 cm^{-1}

As shown in Fig. 7, several marked changes are observed in the spectral region from 1,540 to 1,710 cm^{-1} . These mainly originate from lignin. In this region, only spectral changes for the CML were observed because the Raman spectra of the S_2 , the CML and the CC show similar changes upon [EtPy][Br] treatment. The band intensity decreased at 1,596, 1,620, and 1,656 cm^{-1} , whereas

Fig. 9 Raman mapping on the transverse section of the tracheids before and after treatment with [EtPy][Br] at 120 °C for 0, 24, and 72 h. **a–c** Bright field images of the measured position and the rectangles show the selected regions used for mapping. **d–f** Distribution of lignin (1,581–1,613 cm^{-1}). **g–i** Distribution of the PSs (2,884–2,905 cm^{-1}). *Bright regions* indicate high concentrations of specific chemical compositions, and *dark regions* indicate low concentrations



several new peaks and shoulders appeared at 1,554, 1,590, 1,607, 1,630, and 1,674 cm^{-1} . The new peaks at 1,554, 1,674, and 1,630 cm^{-1} are assigned to *o*-quinone, *p*-quinone, and the C=C bond of stilbene, respectively (Agarwal 1998; Agarwal and Atalla 2000). Therefore, it is possible that the C=C bonds in the coniferyl aldehyde units and in the coniferyl alcohol units decreased and thus quinone and stilbene derivatives were produced upon [EtPy][Br] treatment. Although most of these changes also occurred upon [C2mim][Cl] treatment (Kanbayashi and Miyafuji 2014b), the peak shift at 1,596 cm^{-1} because of an aromatic ring vibration after treatment with [EtPy][Br] was more significant than that after treatment with [C2mim][Cl]. The band at 1,596 cm^{-1} in the spectrum of untreated wood was found to shift to 1,607 cm^{-1} . Additionally, a weak shoulder appeared at 1,590 cm^{-1} . These changes are thought to come from the modification or removal of functional groups related to the aromatic ring. The difference in band shifts after treatment with [EtPy][Br] or [C2mim][Cl] indicates that the interaction of wood with ionic liquids is different. Furthermore, it is suggested that the specific structure of lignin is altered, whereas most of the aromatic rings remain, without change, after treatment with [EtPy][Br] for 72 h.

Region from 2,750 to 3,150 cm^{-1}

All the lignin bands at 2,850, 2,941, and 3,074 cm^{-1} decreased with prolonged treatment for all the cell wall areas. The decrease in the band intensity of the CC was lower than that of the S₂ and the CML. The PSs band intensity at 2,894 cm^{-1} decreased after 24 h, but no change was observed from 24 to 72 h for all the cell wall areas. In this spectral region, many small peaks were detected particularly for the CML and the CC after [EtPy][Br] treatment. The appearance of small peaks may be attributed to C–H stretching in the modified woody components.

Raman mapping

To investigate chemical changes in the cell walls over a larger area during [EtPy][Br] treatment, a time sequential Raman map of lignin and the PSs was obtained. Figure 9a–c shows bright field images of the tracheids in the transverse sections before and after [EtPy][Br] treatment. All the micrographs are images of the same area, and Raman mapping was performed on these cell walls. In the micrographs, the rectangles show the areas selected for mapping. The cell walls gradually became discolored upon

prolonged treatment (Fig. 9a, b). This discoloration of the cell walls supports the point analysis results where the components of the cell walls change their nature upon treatment with [EtPy][Br].

Figure 9d–f, g–i shows Raman images of the distribution of lignin and the PSs before and after treatment with [EtPy][Br], respectively. The band regions from 1,591 to 1,613 cm^{-1} and from 2,884 to 2,905 cm^{-1} in the Raman spectra were selected for the Raman images of lignin and PSs distribution, respectively. The bright areas indicate a high concentration, whereas the dark areas indicate a low concentration. Although the lignin concentration in S_2 decreased significantly with treatment time, the lignin concentration in the CML and the CC only changed slightly. The lignin in the CML and the CC contains many *p*-hydroxyphenyl propane units and it forms a highly condensed structure (Whiting and Goring 1982; Terashima and Fukushima 1988). This lignin structure is highly stable against delignification (Whiting and Goring 1982; Akim et al. 2001). Therefore, the CML and the CC retain high concentrations of lignin after the 72 h treatment. However, the reduction in the amount of lignin in the CML and the CC upon treatment with [EtPy][Br] was greater than that upon treatment with [C2mim][Cl], as reported previously (Kanbayashi and Miyafuji 2014b). Additionally, the concentration of lignin in S_2 decreased homogeneously unlike the case of [C2mim][Cl] treatment. In the Raman image of the 24 h treatment product, it was found that the lignin concentration of the nearby inner layer of the secondary wall (S_3) was higher than that of S_2 . This difference is probably due to differences in the original lignin concentration of the cell wall layers. It has been reported that certain wood species have lignin concentrations in the S_3 of the tracheid that are higher than that of S_2 (Scott and Goring 1970; Donaldson 1987), and Japanese cedar may be one of these species. However, these results were not obtained from S_3 of the non-treated tracheids. This is because the spatial resolution was not sufficient for the observation of S_3 , which is approximately 0.1- μm thick (Harada and Côté 1985). After the 24 h treatment, the thin S_3 swelled because of [EtPy][Br] and it could be distinguished from S_2 . With respect to the PSs, their concentrations decreased significantly after 24 h (Fig. 9h), but no significant changes were observed after 72 h (Fig. 9i). The first decrease in the PSs is likely caused by a reduction in cell wall density because of cell wall swelling.

Conclusions

We investigated the morphological and chemical changes in wood cell walls after treatment with the ionic liquid, [EtPy][Br]. The treatment of Japanese cedar wood with [EtPy][Br] induced a swelling of the wood cell walls

without a significant destruction of the tissue structure or the cellulose crystalline structure. The lignin in the wood cell walls preferentially reacted with [EtPy][Br] and some of its component structures changed. However, the PSs dissolved with difficulty and their nature changed after [EtPy][Br] treatment. Changes in the Raman spectra of the S_2 , the CML, and the CC varied partially during [EtPy][Br] treatment indicating that the reactivity of [EtPy][Br] in wood cell walls is inhomogeneous. Consequently, these new insight into the interaction of wood with ionic liquid at the microscopic cell level provides further comprehension of liquefaction mechanism of woody biomass in ionic liquids. Furthermore, this information will lead to efficient wood disintegration and bioconversion.

Author contribution TK and HM conceived and designed research. TK conducted experiments. TK and HM analyzed data. TK and HM wrote the manuscript. All authors read and approved the manuscript.

Acknowledgments The authors wish to thank the Kyoto Municipal Institute of Industrial Technology and Culture for assistance with the Raman microscopic analyses. This research was partly supported by the Kyoto Prefectural University (KPU) Academic Promotion Fund and a Grant-in-Aid for Scientific Research (c) (25450246) from the JSPS for which the authors are grateful.

References

- Agarwal UP (1998) Assignment of the photo yellowing-related 1675 cm^{-1} Raman/IR band to *p*-quinones and its implications to the mechanism of color reversion in mechanical pulps. *J Wood Chem Tech* 18:381–402
- Agarwal UP (1999) An overview of Raman spectroscopy as applied to lignocellulosic materials. In: Argyropoulos DS (ed) *Advances in lignocellulosics characterization*. TAPPI Press, Atlanta, GA, pp 201–225
- Agarwal UP, Atalla RH (2000) Using Raman spectroscopy to identify chromophores in lignin–lignocellulosics. In: Glasser WG, Northey RA, Schultz TP (eds) *Lignin: historical, biological, and materials perspectives*. ACS Symposium Series, vol 742. American Chemical Society, Washington, DC, pp 250–264
- Agarwal UP, Ralph SA (1997) FT-Raman spectroscopy of wood: identifying contributions of lignin and carbohydrate polymers in the spectrum of black spruce (*Picea mariana*). *Appl Spectrosc* 51:1648–1655
- Agarwal UP, Ralph SA (2008) Determination of ethylenic residues in wood and TMP of spruce by FT-Raman spectroscopy. *Holzforschung* 62:667–675
- Agarwal UP, McSweeney JD, Ralph SA (2011) FT-Raman investigation of milled wood lignins: softwood, hardwood, and chemically modified black spruce lignins. *J Wood Chem Tech* 31:324–344
- Akim LG, Colodette JL, Argyropoulos DS (2001) Factors limiting oxygen delignification of kraft pulp. *Can J Chem* 79:201–210
- Chundawat SPS, Donohoe BS, Sousa LC, Elder T, Agarwal UP, Lu F, Ralph J, Himmel ME, Balan V, Dale BE (2011) Multi-scale visualization and characterization of lignocellulosic plant cell wall deconstruction during thermochemical pretreatment. *Energy Environ Sci* 4:973–984

- Corrales RCNR, Mendes FMT, Perrone CC, Anna C, Souza W, Abud Y, Bon EPS, Ferreira-Leitão V (2012) Structural evaluation of sugar cane bagasse steam pretreated in the presence of CO₂ and SO₂. *Biotechnol Biofuels* 5:36
- Donaldson LA (1987) S₃ lignin concentration in radiate pine tracheids. *Wood Sci Technol* 21:227–234
- Donaldson LA (2001) Lignification and lignin topochemistry—an ultrastructural view. *Phytochemistry* 57:859–873
- Earle MJ, Seddon KR (2000) Ionic liquids. Green solvents for the future. *Pure Appl Chem* 72:1391–1398
- Edwards HGM, Farwell DW, Webster D (1997) FT Raman microscopy of untreated natural plant fibres. *Spectrochim Acta A* 53:2383–2392
- Fort DA, Remsing RC, Swatloski RP, Moyna P, Moyna G, Rogers RD (2007) Can ionic liquids dissolve wood? Processing and analysis of lignocellulosic materials with 1-*n*-butyl-3-methylimidazolium chloride. *Green Chem* 9:63–69
- Freemantle M (1998) Designer solvents—ionic liquids may boost clean technology development. *Chem Eng News* 76:32–37
- Harada H, Côté WA (1985) Structure of wood. In: Higuchi T (ed) Biosynthesis and biodegradation of wood components. Academic Press, Orlando, pp 1–42
- Honglu X, Tiejun S (2006) Wood liquefaction by ionic liquids. *Holzforschung* 60:509–512
- Jansen S, Smets E, Baas P (1998) Vestures in woody plants: a review. *IAWA J* 19:347–382
- Ji Z, Ling Z, Zhang X, Yang GH, Xu F (2014) Impact of alkali pretreatment on the chemical component distribution and ultrastructure of poplar cell walls. *BioResources* 9:4159–4172
- Kanbayashi T, Miyafuji H (2013) Morphological changes of Japanese beech treated with the ionic liquid, 1-ethyl-3-methylimidazolium chloride. *J Wood Sci* 59:410–418
- Kanbayashi T, Miyafuji H (2014a) Comparative study of morphological changes in hardwoods treated with the ionic liquid, 1-ethyl-3-methylimidazolium chloride. *J Wood Sci* 60:152–159
- Kanbayashi T, Miyafuji H (2014b) Raman microscopic analysis of wood after treatment with the ionic liquid, 1-ethyl-3-methylimidazolium chloride. *Holzforschung*. doi:10.1515/hf-2014-0060
- Kilpeläinen I, Xie H, King A, Granstrom M, Heikkinen S, Argyropoulos DS (2007) Dissolution of wood in ionic liquids. *J Agric Food Chem* 55:9142–9148
- Kosan B, Michels C, Meister F (2008) Dissolution and forming of cellulose with ionic liquids. *Cellulose* 15:59–66
- Lee SH, Doherty TV, Linhardt RJ, Dordick JS (2009) Ionic liquid-mediated selective extraction of lignin from wood leading to enhanced enzymatic cellulose hydrolysis. *Biotechnol Bioeng* 102:1368–1376
- Lucas M, Wagner GL, Nishiyama Y, Hanson L, Samayam IP, Schall CA, Langan P, Rector KD (2011) Reversible swelling of the cell wall of poplar biomass by ionic liquid at room temperature. *Bioresour Technol* 102:4518–4523
- Miyafuji H, Suzuki N (2012) Morphological changes in sugi (*Cryptomeria japonica*) wood after treatment with the ionic liquid, 1-ethyl-3-methylimidazolium chloride. *J Wood Sci* 58:222–230
- Miyafuji H, Miyata K, Saka S, Ueda F, Mori M (2009) Reaction behavior of wood in an ionic liquid, 1-ethyl-3-methylimidazolium chloride. *J Wood Sci* 55:215–219
- Mok WSL, Antal MJ Jr (1992) Uncatalyzed solvolysis of whole biomass hemicellulose by hot compressed liquid water. *Ind Eng Chem Res* 31:1157–1161
- Nakamura A, Miyafuji H, Saka S (2010a) Liquefaction behavior of Western red cedar and Japanese beech in the ionic liquid 1-ethyl-3-methylimidazolium chloride. *Holzforschung* 64:289–294
- Nakamura A, Miyafuji H, Saka S (2010b) Influence of reaction atmosphere on the liquefaction and depolymerization of wood in an ionic liquid, 1-ethyl-3-methylimidazolium chloride. *J Wood Sci* 56:256–261
- Piskorz J, Radlein D, Scott DS, Czernik S (1988) Liquid products from the fast pyrolysis of wood and cellulose. In: Bridgewater AV, Kuester JL (eds) Research in thermochemical biomass conversion. Elsevier Applied Science, London, pp 557–571
- Rogers RD, Seddon KR (2003) Ionic liquids—solvents of the future? *Science* 302:792–793
- Schenzel K, Fischer S (2001) NIR FT Raman spectroscopy—a rapid analytical tool for detecting the transformation of cellulose polymorphs. *Cellulose* 8:49–57
- Scott JAN, Goring DAI (1970) Lignin concentration in the S₃ layer of softwoods. *Cellulose Chem Technol* 4:83–93
- Seddon KR (1997) Ionic liquids for clean technology. *J Chem Tech Biotechnol* 68:351–356
- Sheldon R (2001) Catalytic reactions in ionic liquids. *Chem Commun* 23:2399–2407
- Swatloski RP, Spear SK, Holbrey JD, Rogers RD (2002) Dissolution of cellulose with ionic liquids. *J Am Chem Soc* 124:4974–4975
- Taherzadeh MJ, Eklund R, Gustafsson L, Niklasson C, Liden G (1997) Characterization and fermentation of dilute-acid hydrolyzates from wood. *Ind Eng Chem Res* 36:4659–4665
- Terashima N, Fukushima K (1988) Heterogeneity in formation of lignin—XI: an autoradiographic study of the heterogeneous formation and structure of pine lignin. *Wood Sci Technol* 22:259–270
- Viell J, Marquardt W (2011) Disintegration and dissolution kinetics of wood chips in ionic liquids. *Holzforschung* 65:519–525
- Whiting P, Goring DAI (1982) Chemical characterization of tissue fractions from the middle lamella and secondary wall of black spruce tracheids. *Wood Sci Technol* 16:261–267
- Wiley JH, Atalla RH (1987) Band assignments in the Raman spectra of celluloses. *Carbohydr Res* 160:113–129
- Wilkes JS, Zaworotko MJ (1992) Air and water stable 1-ethyl-3-methylimidazolium based ionic liquids. *J Chem Soc, Chem Commun* 13:965–967
- Yamazaki J, Minami E, Saka S (2006) Liquefaction of beech wood in various supercritical alcohols. *J Wood Sci* 52:527–532
- Yokoo T, Miyafuji H (2014) Reaction behavior of wood in an ionic liquid, 1-ethylpyridinium bromide. *J Wood Sci* 60:339–345
- Zhang H, Wu J, Zhang J, He J (2005) 1-Allyl-3-methylimidazolium chloride room temperature ionic liquid: a new and powerful nonderivatizing solvent for cellulose. *Macromolecules* 38: 8272–8277
- Zhang X, Ma J, Ji Z, Yang GH, Zhou X, Xu F (2014) Using confocal Raman microscopy to real-time monitor poplar cell wall swelling and dissolution during ionic liquid pretreatment. *Microsc Res Tech* 77:609–618
- Zhao Y, Wang Y, Zhu JY, Ragauskas A, Deng Y (2008) Enhanced enzymatic hydrolysis of spruce by alkaline pretreatment at low temperature. *Biotechnol Bioeng* 99:1320–1328